JOURNAL OF GEOPHYSICAL RESEARCH, VOL. 111, B12S04, doi:10.1029/2006JB004573, 2006

Memory of the magnetic field applied during cooling in the low-temperature phase of magnetite: Grain size dependence

A. V. Smirnov[1]

Received 15 June 2006; accepted 11 August 2006; published 31 October 2006.

[1] Low-temperature magnetic hysteresis properties of polycrystalline magnetite samples were studied as a function of the magnetic field (H_{FC}) applied during cooling from 300 K to 10 K. The samples ranged in mean grain size from 0.04 to 100 μm, representing mostly single-domain (SD), pseudosingle-domain (PSD), and multidomain (MD) magnetic states. The low-temperature field memory effect, a striking ability of magnetite to memorize the field H_{FC}, is well expressed in PSD magnetite samples (mean grain size ranging from 0.15 to 5 μm). The field memory effect manifests itself as an inflection point of a magnetic hysteresis loop, located in the vicinity of H_{FC}. The effect is greatly reduced in the samples containing larger than 5 μm magnetite grains and is absent in the sample containing large (40 to 200 μm) MD grains. Little or no distortion of hysteresis loops is observed in the samples dominated by SD magnetic grains. The experimental results confirm that the low-temperature field memory effect is a generic property of PSD magnetite and give further support to a phenomenological model in which the field memory originates from an interplay between the magnetic and twin domains in monoclinic magnetite. The observed grain size dependence of the effect implies that the PSD state is a physically distinct magnetic state, rather than simply a manifestation of SD and MD mixing. The distinction is determined by the relative effect of twinning-related crystalline defects on the remagnetization process.

Citation: Smirnov, A. V. (2006), Memory of the magnetic field applied during cooling in the low-temperature phase of magnetite: Grain size dependence, *J. Geophys. Res.*, *111*, B12S04, doi:10.1029/2006JB004573.

1. Introduction

[2] Magnetite (Fe_3O_4) is the most important magnetic mineral in nature, occurring in a great variety of igneous, sedimentary, and metamorphic rocks. The mineral is one of the principal recorders of paleomagnetic information in rocks on the Earth and, possibly, other planets [e.g., *Weiss et al.*, 2002; *Arkani-Hamed*, 2005]. The grain size distribution, oxidation state, and morphology of natural magnetite have been utilized as proxies of climatic, environmental, and biogeochemical processes [e.g., *Kirschvink and Lowenstam*, 1979; *Geiss et al.*, 2004]. Magnetite also has been increasingly used in biotechnology, medicine, the magnetic recording industry, and other fields [e.g., *Alldredge et al.*, 2006; *Li et al.*, 2006].

[3] Magnetite can be identified easily in natural and synthetic materials by low-temperature magnetic measurements, because of its isotropic point at ~135 K [*Syono*, 1965] and its transition from cubic to monoclinic crystalline symmetry at ~120 K (T_V, the Verwey transition) [*Verwey*, 1939]. Low-temperature magnetometry has been utilized for studying grain size distributions [e.g., *Hunt et al.*, 1995], oxidation state [e.g., *Özdemir et al.*, 1993; *Cui et al.*, 1994], and origin [e.g., *Moskowitz et al.*, 1993; *Smirnov and Tarduno*, 2000] of natural magnetite. Interpretations of low-temperature magnetic data, however, ultimately depend on our understanding of the basic magnetic properties of magnetite at cryogenic temperatures.

[4] Although magnetic hysteresis properties of Fe_3O_4 at cryogenic temperatures are of particular interest, because they provide important insights into the crystal and electronic structure of its monoclinic phase as well as the mechanisms of its low-temperature transitions, the corresponding experimental database is small [e.g., *Morish and Watt*, 1958; *Schmidbauer and Schembera*, 1987; *Muxworthy*, 1999; *Özdemir and Dunlop*, 1999; *Kosterov*, 2001]. Still fewer studies investigate the effect of a magnetic field applied during cooling through the transitions (field cooling, FC) on magnetic hysteresis properties of monoclinic magnetite [e.g., *Bickford*, 1953; *Schmidbauer and Keller*, 1996; *Kosterov*, 2001]. In those studies, cooling in a field-free environment (zero field cooling, ZFC) was compared to cooling in very strong (>1.0 T) magnetic fields.

[5] Recently, *Smirnov and Tarduno* [2002a, 2002b] investigated low-temperature hysteresis properties of Fe_3O_4 as a

[1]Department of Geology and Geophysics, Yale University, New Haven, Connecticut, USA.

0148-0227/06/2006JB004573$09.00

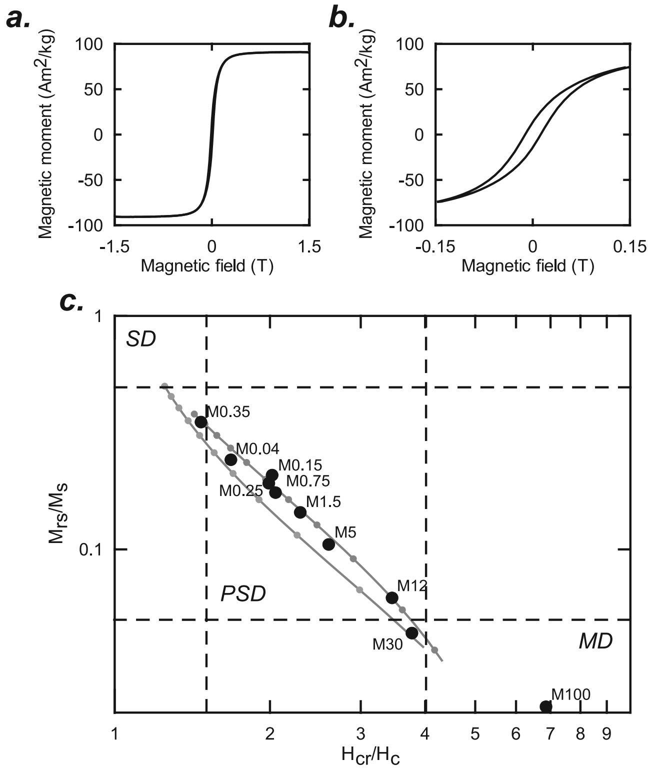

Figure 1. (a) Mass-normalized magnetic hysteresis loop measured from the sample M1.5 at room temperature. (b) A closeup view of the central part of the loop shown in Figure 1a. (c) Day plot [*Day et al.*, 1977]. Abbreviations are H_c, coercivity; H_{cr}, coercivity of remanence; M_{rs}, saturation remanence; and M_s, saturation magnetization; SD, single domain; PSD, pseudosingle-domain; MD, multidomain. Also shown are SD-MD mixture models from *Dunlop* [2002] (grey lines).

function of the magnetic field (H_{FC}) applied during cooling. In contrast to other studies, the authors utilized a wide range of H_{FC} from 0 to 2.5 T. This approach resulted in the discovery of several intriguing phenomena in monoclinic magnetite, including the remarkable effect of memory of the field H_{FC} observed for $H_{FC} < 0.09$ T. The field memory effect is expressed as an inflection point on a magnetic hysteresis loop measured at 10 K after cooling from 300 K to 10 K in the field H_{FC}; the location of this inflection is controlled by the strength of H_{FC}. Application of H_{FC} while passing through the Verwey transition is a necessary condition for the formation of field memory [*Smirnov and Tarduno*, 2002a].

[6] *Smirnov and Tarduno* [2002a] suggested a phenomenological interpretation of field memory as a result of an interplay between the magnetic domain structure and crystallographic twinning in monoclinic magnetite. An important prerequisite for the development of a comprehensive theory of the effect is further accumulation of experimental data. In particular, the results reported by *Smirnov and Tarduno* [2002a, 2002b] are essentially based on only one sample of stoichiometric pseudosingle-domain magnetite.

[7] Here, I report new experimental results on the field memory effect obtained from polycrystalline samples of magnetite characterized by a broad range of grain sizes. The studied samples represented nearly single-domain (SD), pseudosingle-domain (PSD), and multidomain (MD) magnetic states. The goal of this study is twofold. The first goal is to confirm the existence of the low-temperature field memory in different magnetite samples. The second goal is to investigate the grain size dependence of the effect in order to obtain a better insight into the mechanisms of field memory formation.

2. Samples

[8] Ten samples of synthetic polycrystalline magnetite commercially available from Wright Industries Inc and Pfizer companies were studied. Fresh samples were partially oxidized (as was evidenced by completely or partially suppressed Verwey transitions) as a result of their prolonged storage in the air. Before measurements, the samples were reduced in a CO/CO_2 (1:10) atmosphere at 400°C for 3–16 hours to obtain nearly stoichiometric magnetite. The mass-normalized saturation magnetization (M_s^{norm}) measured at room temperature after thermal treatment ranged between 87 and 92 A m^2/kg (Figure 1a), indicating almost complete conversion to pure magnetite [e.g., *Stacey and Banerjee*, 1974]. For additional control, thermal demagnetization of low-temperature saturating isothermal remanent magnetization (LT SIRM) imparted in a 2.5 T direct magnetic field at 20 K was measured between 20 and 300 K using a Quantum Design Magnetic Property Measurement System (MPMS-XL). The sharp Verwey transition observed within ~108–120 K range (Figure 2 and Table 1) for all but one the samples further indicates their stoichiometry [e.g.,

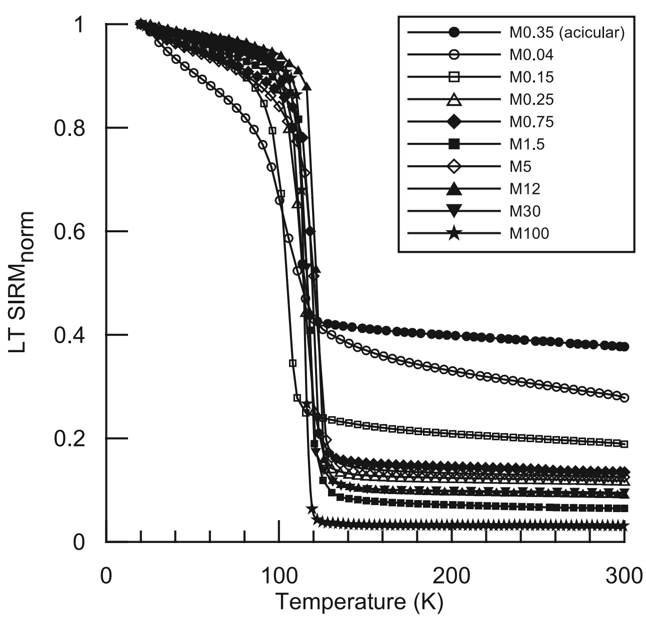

Figure 2. Thermal demagnetization of low-temperature saturation isothermal remanent magnetization (LT SIRM) imparted in a magnetic field of 1.5 T at 20 K. All curves are normalized to the LT SIRM value at 20 K. The samples shown are M0.35 (circles), M0.04 (open circles), M0.15 (open squares), M0.25 (open triangles), M0.75 (diamonds), M1.5 (squares), M5 (open diamonds), M12 (triangles), M30 (inverted triangles), and M100 (stars).

Table 1. Grain Size Distribution and Room Temperature Magnetic Hysteresis Characteristics of the Samples Studied[a]

Sample	d_{mode}, μm	d_{lower}, μm	d_{upper}, μm	T_V, K	M_{rs}/M_s	H_{cr}/H_c
M0.35	0.35	0.2	0.5	114	0.351	1.47
M0.04	0.04	0.02	0.1	101	0.242	1.68
M0.15	0.15	0.03	0.6	108	0.208	2.02
M0.25	0.25	0.1	0.5	116	0.192	1.99
M0.75	0.75	0.3	2.75	118	0.175	2.05
M1.5	1.5	0.5	6.5	118	0.144	2.29
M5	5	2	10	120	0.105	2.6
M12	12	4	20	117	0.062	3.45
M30	30	10	60	116	0.044	3.77
M100	100	40	200	114	0.021	6.86

[a]The parameters d_{mode}, d_{lower}, and d_{upper} are defined in the text. The size of acicular grains in sample M0.35 is measured along their long axes. The Verwey transition temperature (T_V) is defined as the temperature of maximum of the first derivative of a LT SIRM demagnetization curve. H_c, coercivity; H_{cr}, coercivity of remanence; M_{rs}, saturation remanence; and M_s, saturation magnetization.

Özdemir et al., 1993]. The sample M0.04 showed a smeared and shifted to lower temperature transition, suggesting its partial maghemitization.

[9] The grain size and shape distributions of samples were determined by visual inspection of images obtained using a low-voltage, high-resolution LEO 982 scanning electron microscope at the University of Rochester or an XL-30 Environmental Scanning Electron Microscope at Yale University (Figure 3). In all but one sample, magnetite grains were characterized by irregular, nearly equidimensional shape (Figure 3b–3d). One sample (M0.35) contained elongate grains with aspect ratio ranging between ~1:6 and 1:12 (Figure 3a). The grain size distributions for all samples studied are well approximated by a lognormal distribution. Parameters d_{lower}, d_{upper}, and d_{mode} characterize the observed distributions (Table 1). The first two parameters represent the lower and upper limits of grain size in a sample, so that, subjectively, approximately 95% of all the grains in a sample fall between d_{lower} and d_{upper}. The parameter d_{mode} approximately corresponds to the mode of grain size distribution (Figure 4).

[10] To characterize magnetic domain state of the samples, magnetic hysteresis properties (saturation magnetization, M_s; saturation remanence, M_{rs}; coercivity, H_c; coercivity of remanence, H_{cr}) were first measured at room temperature (Table 1), using a Princeton Measurements variable-temperature vibrating sample magnetometer at the Institute of Rock Magnetism (University of Minnesota) and a Princeton Measurement alternating gradient force magnetometer at the University of Rochester. All room temperature hysteresis loops (Figure 1b) and SIRM DC demagnetization curves have a regular shape consistent with unimodal grain size distributions and single mineral compositions [e.g., *Tauxe et al.*, 1996; *Egli*, 2004]. The hysteresis data indicate various magnetic domain behavior of the studied samples (Figure 1c).

[11] Sample M0.35 plots closest to the SD region of the Day plot [*Day et al.*, 1977]. Although grains in this sample

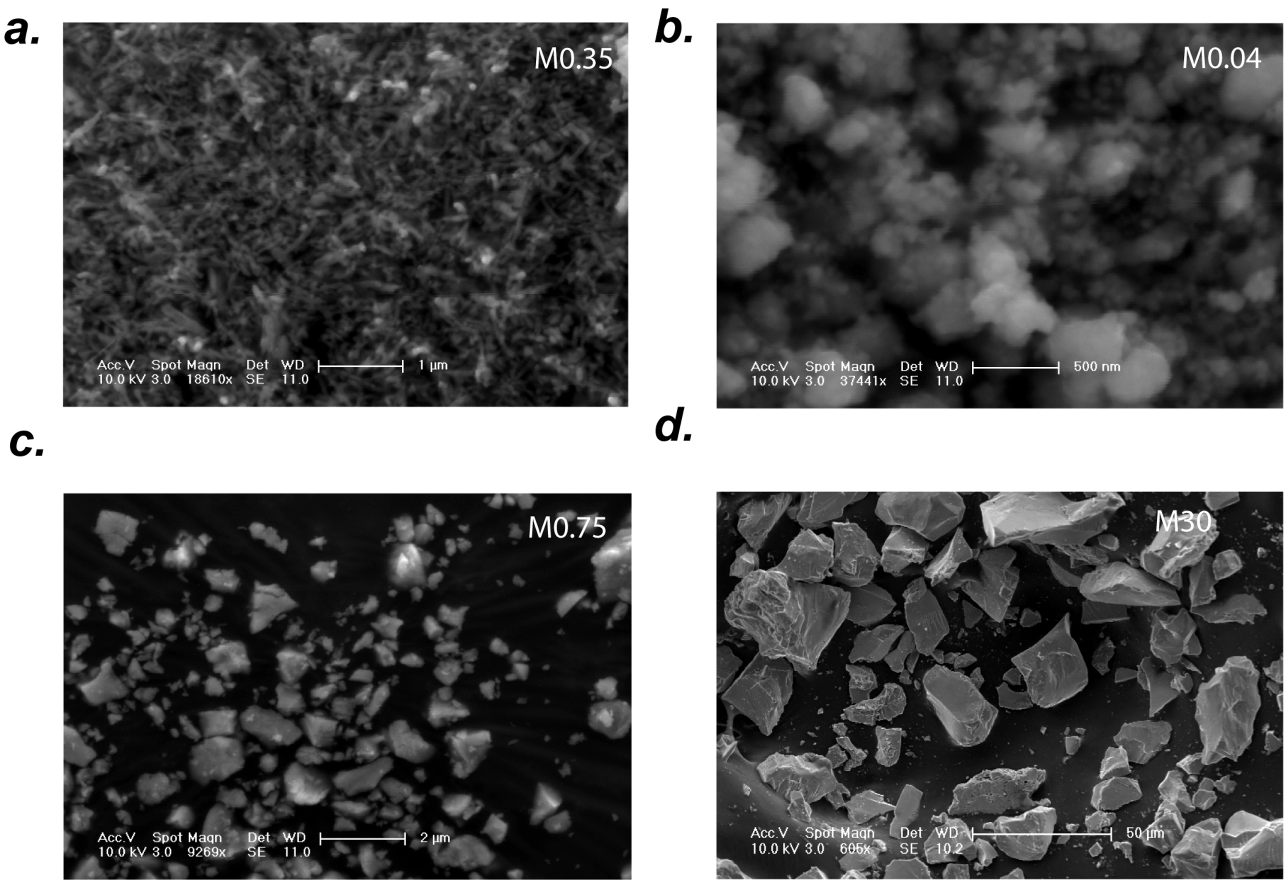

Figure 3. Examples of scanning electron microscope images used to determine the grain and shape distributions of the studied samples: (a) M0.35 (acicular magnetite), (b) M0.04, (c) M0.75, (d) M30.

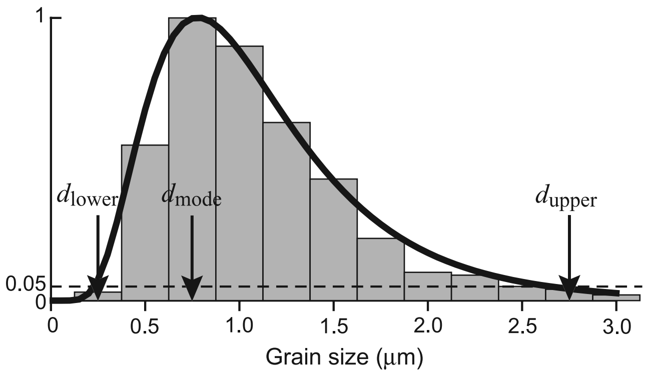

Figure 4. Normalized grain size distribution observed from sample M0.75 (bar plot) and fitted normalized lognormal distribution (solid line). Arrows illustrate how the parameters d_{lower}, d, and d_{mode} were defined. The dashed line shows the 5% probability level.

are larger than the SD threshold for equidimensional magnetite (0.05–0.06 μm; [*Dunlop and Özdemir*, 1997]), their "nearly" SD state is defined by the dominant role of shape anisotropy in the elongate particles [e.g., *Butler and Banerjee*, 1975]. I note that the behavior of elongate magnetic grains may differ from that of idealized, uniformly magnetized SD particles [*Potter and Stephenson*, 2006]. Sample M0.04 also plots relatively close to the SD region, consistent with estimation of the majority of its grains as smaller than the SD threshold.

[12] The M_{rs}/M_s ratios for both the M0.04 and M0.35 samples are lower than the expected theoretical value for noninteracting uniaxial (0.5) or equidimensional (0.866) SD grains [*Dunlop and Özdemir*, 1997], most likely due to magnetostatic interactions between grains [*Sprowl*, 1990]. Additionally, the presence of PSD grains in both samples may lower their M_{rs}/M_s ratios.

[13] Samples M0.15, M0.25, M0.75, M1.5, and M5.0 are characterized by PSD hysteresis behavior, while samples M12, M30, and M100 plot close to or within the MD region of the Day diagram (Figure 1c). Overall, the resultant Day diagram is consistent with observed grain size distributions: samples containing smaller grains plot closer to the SD region of the diagram. I note that all the experimental points lie close to the MD-SD mixing line for magnetite calculated by *Dunlop* [2002].

3. Experimental Procedure

[14] Before low-temperature hysteresis measurements, the samples were demagnetized along three orthogonal axes in an alternating magnetic field of 0.2 T at 300 K. Subsequently, they were cooled to 10 K in a zero magnetic field or in the presence of a magnetic field (H_{FC}) of 0.01, 0.03, or 0.05 T. The actual field strength during ZFC was at least 3 orders of magnitude smaller than the lowest magnetic field applied during field-cooling experiments. At 10 K, saturated (maximum applied field H_{max} = 1.7 T) magnetic hysteresis loops were measured. Although magnetite may not fully saturate in a 1.7 T field at cryogenic temperatures, the difference between measured and true values of M_s has been shown to be only a few percent [*Kosterov*, 2001].

[15] After measurement, the first derivative of the upper branch of a low-temperature hysteresis loop (differential susceptibility, dM/dH) was calculated and plotted versus field, H (Figure 5) to allow more precise identification of hysteresis loop distortion.

4. Experimental Results

[16] Figures 6 and 7 show the dM/dH curves measured after cooling in zero field and in the fields H_{FC} of 0.01, 0.03, and 0.05 T (hereafter, the dM/dH_{ZFC}; $dM/dH_{0.01T}$; $dM/dH_{0.03T}$; and $dM/dH_{0.05T}$). To facilitate comparison of dM/dH for different samples, all the curves measured from a single sample were normalized by the maximum value of its $dM/dH_{0.05T}$ curve.

[17] No distortions were observed on the ZFC and FC loops measured from acicular magnetite (M0.35) (Figure 6a). Independent of H_{FC}, all four dM/dH curves have a regular shape, characterized by a single maximum at a negative field with smooth ascending (as H decreases from its maximum positive value) and descending slopes. However, increase of H_{FC} results in a relative increase of dM/dH maxima (Figure 6a).

[18] Sample M0.04 shows distorted low-temperature magnetic hysteresis loops after both zero field cooling and cooling in 0.01 T. The distortion is expressed as a bump on the ascending side of corresponding dM/dH curves, located in the negative field range (Figure 6b). Much weaker bumps, observed on the $dM/dH_{0.03T}$ and $dM/dH_{0.05T}$ curves, were located roughly at the field H_{FC} (Figure 6b).

[19] All pseudosingle-domain samples (M0.15, M0.25, M0.75, M1.5 and M5) manifest distinct distortions on magnetic hysteresis loops measured after field cooling, located in close proximity to H_{FC}. The distortions were expressed either as local maxima or as plateaus on the ascending slopes of dM/dH (Figures 6c–6f and 7a). Interestingly, for all PSD samples, zero field cooling also result in distorted hysteresis loops, expressed as a zone of constant or

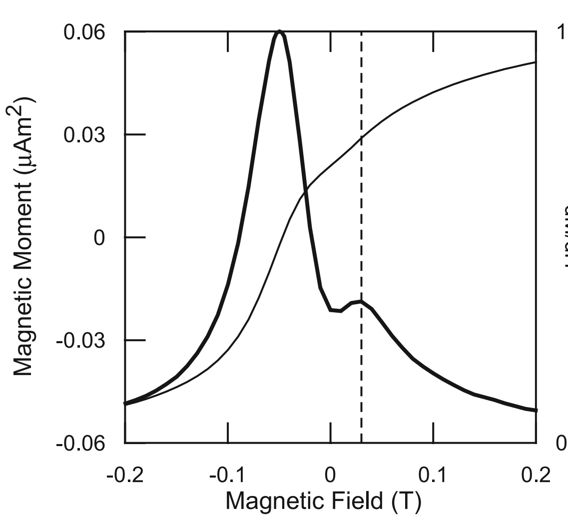

Figure 5. Magnetic hysteresis loop (central part) measured from the sample M1.5 at 10 K after cooling in a 0.03 T magnetic field (dashed line). Thicker solid line shows the normalized first derivative of the upper branch of the loop.

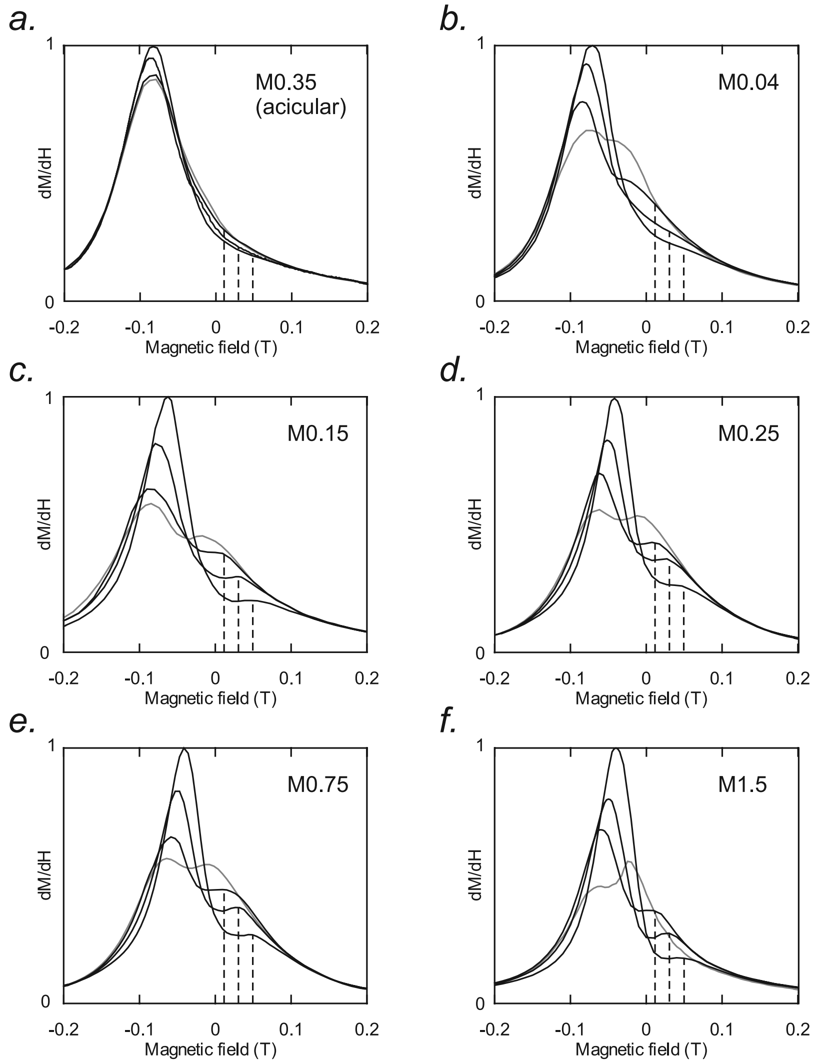

Figure 6. First derivatives of hysteresis loops (upper branches only) measured at 10 K after zero field cooling (grey curve), and after cooling (solid curves) in fields of 0.01, 0.03, and 0.05 T (shown by dashed lines). (a) M0.35 (acicular magnetite), (b) M0.04, (c) M0.15, (d) M0.25, (e) M0.75, (f) M1.5.

decreased differential susceptibility (dM/dH_{ZFC}) at H < 0 (Figures 6c–6f and 7a; grey line).

[20] No local dM/dH maxima or plateaus are observed in the samples containing larger grains. However, the $dM/dH_{0.03T}$ and $dM/dH_{0.05T}$ curves of sample M12 manifest a noticeable bend in the vicinity of H_{FC} (Figure 7b). The $dM/dH_{0.03T}$ and $dM/dH_{0.05T}$ curves of sample M30 display similar but less well-expressed behavior (Figure 7c). Sample M100, containing the largest grain size population, manifests no noticeable distortions of low-temperature hysteresis loops (Figure 7d).

5. Discussion

[21] The most important outcome of this study is confirmation of the existence of low-temperature field memory effect in various magnetite samples, further strengthening the conclusions of *Smirnov and Tarduno* [2002a, 2002b]. Field memory is best expressed in pseudosingle-domain magnetites with the mean grain size ranging from 0.15 to 5 μm.

[22] The obtained results reveal a dependence of field memory on the magnetic domain state of magnetite. The effect is practically absent in a sample with a large proportion of grains smaller than the SD threshold of Fe_3O_4. Furthermore, the effect is not observed in a sample dominated by elongate, supposedly SD grains. The manifestation of field memory is greatly reduced for samples containing larger than 5 μm grains, and the effect is not observable in a sample containing large (40 to 200 μm, mean size $\sim$100 μm) multidomain grains.

[23] *Smirnov and Tarduno* [2002a, 2002b] proposed that the phenomenon of low-temperature field memory originates from a dynamic interaction between the crystallographic and magnetic domain structures in monoclinic magnetite. Lowering of crystal symmetry below T_V results in the appearance of ferroelastic domains, or twins, to reduce spontaneous strain [e.g., *Chikazumi et al.*, 1971; *Abe et al.*, 1976; *Medrano et al.*, 1999]. Within a ferroelastic domain, the direction of c axis is constant. It has been universally accepted that in the absence of external enforcement (e.g., a magnetic field)

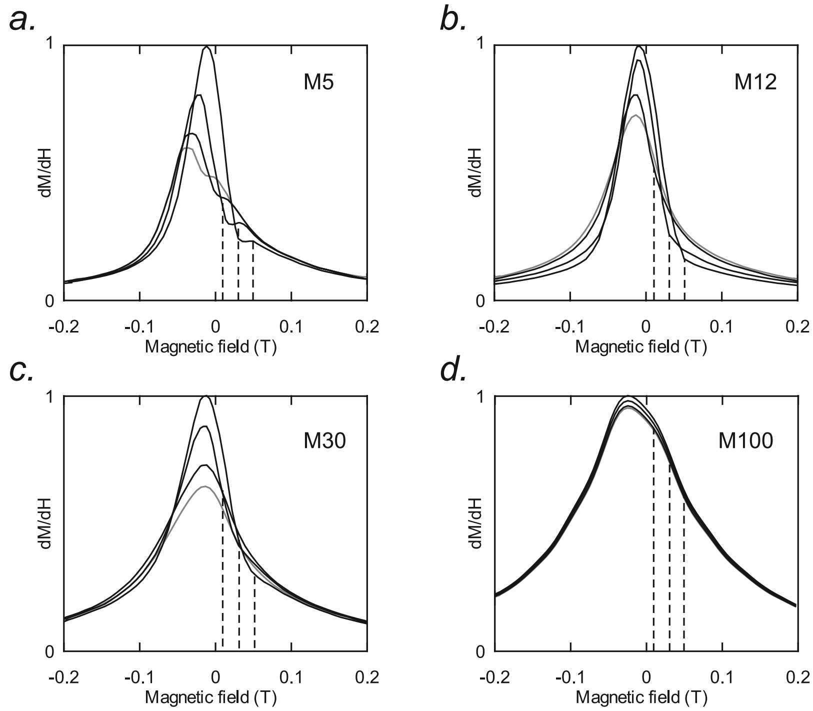

Figure 7. First derivatives of hysteresis loops (upper branches only) measured at 10 K after zero field cooling (grey curve), and after cooling (solid curves) in fields of 0.01, 0.03, and 0.05 T (shown by dashed lines). (a) M5, (b) M12, (c) M30, (d) M100.

during cooling, the monoclinic c axis may develop in any of the cube edge orientations with equal probability. However, application of a strong magnetic field (>100 mT) during cooling prevents twinning by setting all c axes along the cubic [001] direction closest to the magnetic field [e.g., *Calhoun*, 1954]. Furthermore, the experimental study by *Smirnov and Tarduno* [2002a] strongly suggests that even magnetic fields H_{FC} lower than 100 mT exert some control on twinning.

[24] *Smirnov and Tarduno* [2002a] suggested that the distribution of monoclinic twin boundaries is controlled by the configuration of magnetic domains existing in a grain upon passing through the Verwey transition (e.g., as a result of magnetostriction-induced strain in the vicinity of a magnetic domain wall). After a magnetic domain wall is moved by remagnetization from its position previously determined by cooling in a field H_{FC} (including $H_{FC} = 0$), this location is "memorized" by the overall configuration of twinning-induced irregularities of the crystalline lattice. Zones of elevated strain and dislocations associated with twin boundaries and junctions may create additional potential energy barriers, which hinder the motion of the magnetic domain walls during the field cycling used in magnetic hysteresis measurements at low temperatures [e.g., *Träuble*, 1969; *Özdemir and Dunlop*, 1999]. Consequently, the field memory effect reflects inhibited remagnetization near the field of cooling (H_{FC}) value, which is expressed in a distortion of a hysteresis loop.

[25] This phenomenological model successfully accounts for not only the field memory and its properties (e.g., the uniaxial anisotropy), but also other intriguing properties of monoclinic magnetite, such as a nonmonotonic dependence of the M_{rs}/M_s ratio on the field H_{FC}, and nonmonotonic field dependence of low-temperature transitional remanent magnetization [*Smirnov and Tarduno*, 2002a]. While a rigorous theory of these effects remains to be developed, the experimental data presented here are consistent with the model of *Smirnov and Tarduno* [2002a] and provide an additional insight into the mechanism of low-temperature field memory.

[26] Importantly, manifestation of the effect decreases with increasing grain size in a sample (Figures 6 and 7). I suggest that the grain size dependence reflects changes in the relative contribution of magnetic domain walls, which motion is affected by the twinning-induced defects, to the remagnetization process. I speculate that a more or less one-to-one correspondence exists between the twin and magnetic domains (or boundaries) in smaller PSD particles. As a result, motion of most of the magnetic domain walls is influenced by the twinning-induced crystalline defects, resulting in a strong field memory effect.

[27] In contrast, in large, truly MD particles, only a small fraction of magnetic domain walls will be affected by twinning, so that any signal from these walls will be overwhelmed by that from "normal" magnetic domain walls; hence no field memory is observed. Such a situation can arise, for instance, if the size of ferroelastic domains is much larger than that of magnetic domains. Consequently, each MD grain is divided by twinning into several smaller, but still multidomain volumes, in which remagnetization is not affected by twinning.

[28] Another important observation is that the samples characterized by well-expressed field memory also manifest a distortion of loops measured after ZFC, expressed as a zone of constant or decreased differential susceptibility

(Figures 6c–6f and 7a). I suggest that such a behavior is also caused by the twinning-induced defects, inhibiting remagnetization. In principle, the configuration of twins after ZFC should be random, solely defined by the minimization of elastic energy. Therefore the zone of abnormal differential susceptibility should be located in the vicinity of zero field on corresponding dM/dH_{ZFC} curves. However, the zone is shifted to negative fields (Figures 6 and 7). The cause of this shift is unclear and requires further investigation. I speculate that it may be related to the possible effect of the initial (room temperature) magnetic state of a sample on the distribution of monoclinic c axes after ZFC, as suggested by recent experimental and theoretical studies [*Kosterov*, 2001; *Muxworthy and Williams*, 2006].

[29] The model of *Smirnov and Tarduno* [2002a] implies that field memory effect cannot form in truly single domain grains, because no domain walls exist to give rise to field memory. Unfortunately, because of the very narrow range of single-domain behavior in magnetite, it is difficult to obtain a synthetic sample of truly SD equidimensional magnetite [e.g., *Schmidbauer and Schembera*, 1987]. However, I feel that samples M0.35 and M0.04, although nonideal, provide a good proxy for the processes governing low-temperature magnetic behavior of ideal SD grains.

[30] Indeed, SEM analyses indicate that most of sample M0.04 grains should be in single-domain state (Figure 3b and Table 1) and hence should not generate field memory effect. This is consistent with only small hysteresis loop distortions observed from this sample (Figure 6b). Most likely, these distortions are due to the presence of grains larger than the SD threshold. In such grains, the distribution of spin moments may be nonuniform and remagnetization may occur in a more complicated way than coherent rotation [e.g., *Dunlop*, 1977; *Schmidtbauer and Schembera*, 1987]. I suggest that the remagnetization of such metastable SD grains [*Dunlop and Özdemir*, 1997] may be influenced by the distribution of twin domains (if any), resulting in a slightly distorted ZFC loop, in a fashion similar to its PSD counterparts.

[31] A field of 0.01 T appears to be insufficient to significantly change the twin configuration in comparison with that formed after ZFC, resulting in the overall similarity of the $dM/dH_{0.01T}$ and dM/dH_{ZFC} curves (Figure 6b). It is also likely that sample M0.04 contains even larger grains in which remagnetization occurs through magnetic domain wall displacements. Such grains may be responsible for the minor inflections on the $dM/dH_{0.03T}$ and $dM/dH_{0.05T}$ curves, hinting at field memory effect. Although the small grain size appears to be the major factor controlling magnetic properties of sample M0.04, the low-temperature effects in the sample may also be attenuated by maghemitization, pervasive in small magnetite grains [e.g., *Dunlop and Özdemir*, 1997] (Figure 2).

[32] Acicular magnetite sample M0.35 contains grains comparable in size to those in some of the PSD samples (Table 1). Therefore it is reasonable to assume that an acicular grain is subdivided into several twin domains below T_V. Because the magnetic behavior of these twin domains will be controlled by strong uniaxial magnetocrystalline anisotropy [*Carter-Stiglitz et al.*, 2002], they will behave as SD grains, prohibiting the emergence of field memory (no magnetic domain walls exist to move through the twinning-induced barriers). However, the difference in the dM/dH curves corresponding to different H_{FC} fields (Figure 6a) cannot be explained by this mechanism. This variation is most likely caused by PSD grains present in the sample M0.35. In addition, the nonideal SD behavior of elongate magnetite particles [*Potter and Stephenson*, 2006] may contribute to the difference.

[33] The observations reported in this paper and elsewhere [e.g., *Özdemir and Dunlop*, 1999; *Kosterov*, 2001; *Smirnov and Tarduno*, 2002a, 2002b] strongly suggest that twinning plays an important role in defining the low-temperature hysteresis properties of magnetite. An important question remains: what is the minimum size of a monoclinic magnetite grain in which transformational twinning may occur? It has been suggested that the basic principles governing the formation of twin domains are principally the same as in the formation of ferromagnetic domains [e.g, *Khachaturyan*, 1983; *Roitburd*, 1988]. While the latter emerge from a reduction of magnetostatic energy through the arrangement of magnetization directions, the former reduce the strain energy by the mutual arrangement of the crystallographic variants [e.g., *Zhang and Soffa*, 1992]. If this is correct, then a minimal grain size allowing twinning should exist by analogy with the ferromagnetic SD threshold. However, to the best of my knowledge, no such estimate exists for magnetite. Experimentally, transformational twinning at a scale as small as 10–100 nm was observed in Fe-Pd and Fe-Pt alloys [*Zhang and Soffa*, 1992].

[34] If field memory effect is intimately associated with twinning, then the presented results indicate that the latter occurs in magnetite grains as small as 0.15 μm and, possibly, even smaller. A more definitive answer to this problem, however, can be provided only by direct microscopic observation.

6. Conclusions

[35] The experimental results show that the low-temperature field memory effect is a generic property of magnetite, expressed within a $\sim$0.15–5 μm grain size range. The observed grain size dependence of the effect hints that, at temperatures below the Verwey transition, a distinction can be made between the pseudosingle-domain and "true" multidomain magnetic states. Consequently, it implies that PSD behavior is indeed a distinct physical reality rather than a manifestation of a mixture of SD and MD grains [e.g., *Dunlop*, 2002]. Further refinement of the grain size range in which the effect is observed will require samples characterized by narrow grain size distributions and well-controlled grain shape and spacing. In spite of many technological difficulties, the fabrication of such samples is within reach as promised by recent advances in nanoengineering [e.g., *Wang et al.*, 2004].

[36] While a good agreement of presented observations with the phenomenological model of *Smirnov and Tarduno* [2002a, 2002b] strongly supports the validity of the latter as a general interpretive scheme, a comprehensive theory of the field memory and related effects is still to be developed. Any theoretical advance in this direction should incorporate a critical role of crystallographic controls on magnetic hysteresis properties of monoclinic magnetite indicated by the experimental data. Such a theory would be useful for better understanding not only the low-temperature hysteresis prop-

erties of magnetite, but also properties of other compounds of geophysical importance (e.g., perovskites), in which a similar relationship between magnetic and crystallographic properties could be anticipated at ambient temperature [e.g., *Huang et al.*, 2006].

[37] **Acknowledgments.** I thank John Tarduno for useful discussions. I also thank Andrei Kosterov and Pavel Doubrovine for helpful comments. I am grateful to the Institute for Rock Magnetism (University of Minnesota) for a Visiting Fellowship. Funds for the IRM are provided by the National Science Foundation (NSF) Instruments and Facilities Program and by the University of Minnesota. Overall support for this research was provided by the NSF and the David and Lucile Packard Foundation.

References

Abe, K., Y. Miyamoto, and S. Chikazumi (1976), Magnetocrystalline anisotropy of low temperature phase of magnetite, *J. Phys. Soc. Jpn.*, *41*, 1894–1902.

Alldredge, L. M. B., R. V. Chopdekar, B. B. Nelson-Cheeseman, and Y. Suzuki (2006), Complex oxide-based magnetic tunnel junctions with nonmagnetic insulating barrier layers, *J. Appl. Phys.*, *99*, 08K303.

Arkani-Hamed, J. (2005), On the possibility of single-domain/pseudosingle-domain magnetic particles existing in the lower crust of Mars: Source of the strong magnetic anomalies, *J. Geophys. Res.*, *110*, E12009, doi:10.1029/2005JE002535.

Bickford, L. R. (1953), The low temperature transformation in ferrites, *Rev. Mod. Phys.*, *25*, 75–79.

Butler, R. F., and S. K. Banerjee (1975), Theoretical single-domain grain-size range in magnetite and titanomagnetite, *J. Geophys. Res.*, *80*, 4049–4058.

Calhoun, B. A. (1954), Magnetic and electric properties of magnetite at low temperatures, *Phys. Rev.*, *94*, 1577–1585.

Carter-Stiglitz, B., M. Jackson, and B. Moskowitz (2002), Low-temperature remanence in stable single domain magnetite, *Geophys. Res. Lett.*, *29*(7), 1129, doi:10.1029/2001GL014197.

Chikazumi, S., K. Chiba, K. Suzuki, and T. Yamada (1971), Electron microscopic observation of low temperature phase of magnetite, in *Ferrites: Proceedings of the International Conference*, edited by Y. Hoshino et al., pp. 141–143, Univ. of Tokyo Press, Tokyo.

Cui, Y., K. L. Verosub, and A. P. Roberts (1994), The effect of low temperature oxidation on large multi-domain magnetite, *Geophys. Res. Lett.*, *21*, 757–760.

Day, R., M. Fuller, and V. A. Schmidt (1977), Hysteresis properties of titanomagnetites: Grain-size and compositional dependence, *Phys. Earth Planet. Inter.*, *13*, 260–267.

Dunlop, D. J. (1977), The hunting of the 'psark', *J. Geomagn. Geoelectr.*, *29*, 293–318.

Dunlop, D. J. (2002), Theory and application of the Day plot (M_{rs}/M_s versus H_{cr}/H_c): 1. Theoretical curves and tests using titanomagnetite data, *J. Geophys. Res.*, *107*(B3), 2056, doi:10.1029/2001JB000486.

Dunlop, D. J.. and Ö. Özdemir (1997), *Rock Magnetism: Fundamentals and Frontiers*, 573 pp., Cambridge Univ. Press, New York.

Egli, R. (2004), Characterization of individual rock magnetic components by analysis of remanence curves, 1. Unmixing natural sediments, *Studia Geophys. Geod.*, *48*, 391–446.

Geiss, C. E., C. W. Zanner, S. K. Banerjee, and M. Joanna (2004), Signature of magnetic enhancement in a loessic soil in Nebraska, United States of America, *Earth Planet. Sci. Lett.*, *228*, 355–367.

Huang, Y. H., M. Karppinen, H. Yamauchi, and J. B. Goodenough (2006), Systematic studies on effects of cationic ordering on structural and magnetic properties in Sr_2FeMoO_6, *Phys. Rev. B*, *73*, 104408.

Hunt, C. P., S. K. Banerjee, J. Han, P. A. Solheid, E. Oches, W. Sun, and T. Liu (1995), Rock-magnetic proxies of climate change in the loess-palaeosol sequences of the western Loess Plateau of China, *Geophys. J. Int.*, *123*, 232–244.

Khachaturyan, A. G. (1983), *Theory of Structural Transformations in Solids*, 574 pp., John Wiley, Hoboken, N. J.

Kirschvink, J. L., and H. A. Lowenstam (1979), Mineralization and magnetization of chiton teeth: Paleomagnetic, sedimentologic, and biologic implications of organic magnetite, *Earth Planet. Sci. Lett.*, *44*, 193–204.

Kosterov, A. A. (2001), Magnetic hysteresis of pseudo-single-domain and multidomain magnetite below the Verwey transition, *Earth Planet. Sci. Lett.*, *186*, 245–253.

Li, G. X., S. H. Sun, and S. X. Wang (2006), Spin valve biosensors: Signal dependence on nanoparticle position, *J. Appl. Phys.*, *99*, 08P107.

Medrano, C., M. Schlenker, J. Baruchel, J. Espeso, and Y. Miyamoto (1999), Domains in the low-temperature phase of magnetite from synchrotron-radiation X-ray topographs, *Phys. Rev. B.*, *59*, 1185–1195.

Morish, A. H., and L. A. K. Watt (1958), Coercive force of iron oxide micropowders at low temperatures, *J. Appl. Phys.*, *29*, 1029–1033.

Moskowitz, B. M., R. B. Frankel, and D. A. Bazylinski (1993), Rock magnetic criteria for the detection of biogenic magnetite, *Earth Planet. Sci. Lett.*, *120*, 283–300.

Muxworthy, A. R. (1999), Low-temperature susceptibility and hysteresis of magnetite, *Earth Planet. Sci. Lett.*, *169*, 51–58.

Muxworthy, A. R., and W. Williams (2006), Low-temperature cooling behavior of single-domain magnetite: Forcing of the crystallographic axes and interactions, *J. Geophys. Res.*, *111*, B07103, doi:10.1029/2006JB004298.

Özdemir, Ö., and D. J. Dunlop (1999), Low-temperature properties of a single crystal of magnetite oriented along principal magnetic axes, *Earth Planet. Sci. Lett.*, *165*, 229–239.

Özdemir, Ö., D. J. Dunlop, and B. M. Moskowitz (1993), The effect of oxidation on the Verwey transition in magnetite, *Geophys. Res. Lett.*, *20*, 1671–1674.

Potter, D. K., and A. Stephenson (2006), The stable orientations of the net magnetic moment within single-domain particles: Experimental evidence for a range of stable states and implications for rock magnetism and palaeomagnetism, *Phys. Earth Planet. Inter.*, *154*, 337–349.

Roitburd, A. L. (1988), Thermodynamics of polydomain phases, in *Phase Transformations 87*, edited by G. W. Lorimer, p. 414, Inst. of Metals, London.

Schmidbauer, E., and R. Keller (1996), Magnetic properties and rotational hysteresis of Fe_3O_4 and g-Fe_2O_3 particles $\sim$250 nm in diameter, *J. Magn. Magn. Mater.*, *152*, 99–108.

Schmidbauer, E., and N. Schembera (1987), Magnetic hysteresis properties and anhysteretic remanent magnetization of spherical Fe_3O_4 particles in the grain size range 60–160 nm, *Phys. Earth Planet. Inter.*, *46*, 77–83.

Smirnov, A. V., and J. A. Tarduno (2000), Low-temperature magnetic properties of pelagic sediments (Ocean Drilling Program Site 805C): Tracers of maghemitization and magnetic mineral reduction, *J. Geophys. Res.*, *105*, 16,457–16,471.

Smirnov, A. V., and J. A. Tarduno (2002a), Magnetic field control of the low-temperature magnetic properties of stoichiometric and cation-deficient magnetite, *Earth Planet. Sci. Lett.*, *194*, 359–368.

Smirnov, A. V., and J. A. Tarduno, (2002b). Magnetite reveals ambient field strength at low temperatures, *Eos Trans. AGU*, *83*(29), 309, 315–316.

Sprowl, D. R. (1990), Numerical estimation of interactive effects in single-domain magnetite, *Geophys. Res. Lett.*, *17*, 2009–2012.

Stacey, F. D., and S. K. Banerjee (1974), *The Physical Principles of Rock Magnetism*, 195 pp., Elsevier, New York.

Syono, Y. (1965), Magnetocrystalline anisotropy and magnetostriction of Fe_3O_4-Fe_2TiO_4 series—With special application to rock magnetism, *Astrophys. J. Geophys.*, *4*, 71–143.

Tauxe, L., T. A. T. Mullender, and T. Pick (1996), Potbellies, wasp-waists, and superparamagnetism in magnetic hysteresis, *J. Geophys. Res.*, *101*, 571–583.

Träuble, H. (1969), The influence of crystal defects on magnetization processes in ferromagnetic single crystals, in *Magnetism and Metallurgy*, edited by A. E. Berkowitz, and E. Kneller, pp. 622–687, Elsevier, New York.

Verwey, E. J. W. (1939), Electron conduction of magnetite (Fe_3O_4) and its transition point at low temperatures, *Nature*, *144*, 327–328.

Wang, J., Z. M. Peng, Y. J. Huang, and Q. W. Chen (2004), Growth of magnetite nanorods along its easy-magnetization axis of [110], *J. Cryst. Growth*, *263*, 616–619.

Weiss, B. P., H. Vali, F. J. Baudenbacher, J. L. Kirschvink, S. T. Stewart, and D. L. Shuster (2002), Records of an ancient Martian magnetic field in ALH84001, *Earth Planet. Sci. Lett.*, *201*, 449–463.

Zhang, B., and W. A. Soffa (1992), Magnetic domains and coercivity in polytwinned ferromagnets, *Phys. Status Solidi*, *131*, 707–725.

A. V. Smirnov, Department of Geology and Geophysics, Yale University, P.O. Box 208109, New Haven, CT 06511, USA. (aleksey.smirnov@yale.edu)